



## Design and fabrication of a new micro-power scaled electromagnetic harvester

Büşra Mutlu

Gazi University, Technology Faculty, Department of Electrical and Electronics Engineering, TR-06500 Beşevler, Ankara, Turkey, E-mail: bussmutlu@gmail.com, orcid.org/0000-0003-2807-2164

Erol Kurt

Gazi University, Technology Faculty, Department of Electrical and Electronics Engineering, TR-06500 Beşevler, Ankara, Turkey, E-mail: ekurt@gazi.edu.tr, orcid.org/0000-0002-3615-6926

Nicu Bizon

University of Pitesti, 1 Targu din Vale, Arges, 110040 Pitesti, Romania, E-mail: nicubizon@yahoo.com, orcid.org/0000-0001-9311-7598

Jose Manuel Lopez-Guede

Basque Country University (UPV/EHU), Faculty of Engineering, Department of Engineering Systems and Automatics, Vitoria-Gasteiz, Spain, E-mail: jm.lopez@ehu.es, orcid.org/0000-0002-5310-1601

Arrived: 17.04.2019 Accepted: 05.05.019 Published: 30.06.2019

**Abstract:** In the present study, a new micro-power scaled electromagnetic (EM) harvester is designed and fabricated. The device has an innovative magnetic flux varying mechanism with two cylindrical Nb magnets and a central core moving inside the magnets back and forth. The system harvest electricity from the linear oscillations by the help of a spring attached at the bottom part of the core. The device requires only one spring and a second linear-laminated core closes the flux outside of the magnets in order to lower the reluctance of the system. The device is 6 cm in length and 2.4 cm in width in cylindrical geometry as a compact and stable geometry. The experimental verifications have proven that it can generate up to  $U = 7.76$  mV output voltage depending on the oscillation frequency. The maximal output power has been measured as  $P = 32$   $\mu$ W for 44 Hz frequency with the resistive load  $R_L = 0.2$  Ohm. The power density  $p = 1.17$   $\mu$ W/cm<sup>3</sup> has been obtained, experimentally.

**Keywords:** Electromagnetic harvester, Power, Flux, Core

Cite this paper as: Mutlu, B., Kurt, E., Bizon, N. and Lopez Guede J.M. Design and Fabrication of a New Micro-Power Scaled Electromagnetic Harvester, Journal of Energy Systems 3(2); (2019); 51-66, DOI: 10.30521/jes.554900

## 1. INTRODUCTION

After the pioneering study of Faraday, energy harvesting became the most applicable area of the engineering. After the invention of the electrical potential difference on a conducting wire can be achieved by a moving magnetic field, it has been the main idea for the electrical conversion from any mechanical system. Mainly that idea was sounded as Faraday's law to explain the electromotive force (EMF) and its magnetic related nature [1]. Modern industry has found new applications on the electromagnetism of moving bodies, which aims to generate electricity for small-scale systems, especially for compact systems for instance, alarms, clocks, sensorless nodes, attenuators, tire pressure control and other automotive sensing units [2-4].

In the literature, the studies on experimental and simulation studies on harvesters get much interest to apply the above-mentioned structures: As the main rule, the magnetic flux and air gap are vital to achieve the maximal voltage [5,6]. In addition, the number of coil turns, electromagnetic (EM) damping and velocity of the moving part (i.e. magnet or coil) important role to get the maximal power [1]. Voltage and power are vital quantities to determine the harvesting from a harvester. In the EM harvesters, power obtained from the harvester is governed by the electrical load [7,8]. Indeed, the output terminals of the harvesters may provide better power when the impedances of the harvester and the electrical load are equalized [7,8]. From electrical point of view, the maximal power idea defines the exact power point for the maximal value. Indeed, it aims to consider the electrical load where the multiplication of current and voltage becomes maximal, thereby many tests are applied to the devices in order to optimize the system. In that respect, the optimization gets much intention because of the exploration of the system parameters including electrical load, air gap, core geometry, permeability, mass, winding geometry and frequency depending on the device features.

The present technology has improved high magnetic density materials, which are used for cores and permanent magnets. The magnets can be made from the materials exhibiting magnetism effect after the application of magnetization by using the electromagnets or permanent magnets. In that respect, the ferromagnetic materials are apart from the ferromagnetic ones, because they contain opposite magnetic moments. However, the magnitude of these moments is unequal and that causes net magnetic field inside the material. Indeed, such ferrimagnetics take interest because of their high electrical resistance and the eddy current effects are minimized in such materials.

There exist different types of magnets: Alnico, neodymium iron boron, samarium cobalt and ceramic. Each magnet has different feature. Among them, the highest energy is achieved from NdFeB magnets, however these rare-earth magnets suffer from low temperatures. Indeed, the maximal temperature in the applications can be around 120 °C. Besides, they have also poor corrosion resistance. For Alnico material, the maximal temperature can be increased up to 550 °C. This value is well beyond the NdFeB magnets, whereas the flux density is lowered to 130 mT. The same quantity is 3.5 times lower for NdFeB material. This discussion motivates the scientists to develop alternative cooling mechanisms for the harvesters.

According to the literature, the relation of generated power and the harvester size is an important issue. For instance, in the mechanical vibration - driven ones, the available mechanical power is strictly dependent on the mass movement in a certain distance. If a core tip is considered relatively, its movement from the equilibrium point of the device makes sense in that regard. The movement produces parasitic and EM damping quantities. Typically, if the device dimension is decreased, the generated electrical power is drastically reduced due to EM damping as discussed in Ref. [9]. The second quantity - parasitic damping is produced by the combination of material and air frictions. Then, it becomes the main limiter for the harvester displacement if the geometries of core and windings are not limiting the locations.

Amirtharajah and his co-worker [10] designed a harvester consisting of a cylindrical housing winding in 1998. In their work, a cylindrical mass was put into a spring and fixed to one tip. A permanent magnet was attached to the other tip of the housing with a mass. This mass also has a coil to oscillate free in the vertical direction. The moving mass causes to cut the magnetic flux and a certain EMF was obtained between the terminals of the coil. The harvested peak voltage was found as 0.18 V, which was too low to be rectified by a standard diode and only the small proportion of power (i.e. 400  $\mu\text{W}$ ) could be harvested inside 2 cm movement. In other study, El-Hami et al [11] considered a cantilever beam type system with a C – shaped core. In the design, a magnet pair was attached to two inner sides of the core as freely vibrating with the cantilever inside a stable coil. The total harvester volume was 240  $\text{mm}^3$  in their work and power of 0.53 mW was harvested for 322 Hz oscillations inside 25  $\mu\text{m}$  movement. The measured voltage was 0.15 V in their experiments. Glynne-Jones and his co-workers [12] applied a different configuration: Four magnets and a fixed coil were used in two cantilever structures. The total harvester volume was 3.15  $\text{cm}^3$  and the optimum operation frequency was found as 106 Hz. The output voltage was measured as 1 V. They also located the harvester onto a car engine and obtained the maximal peak power of 4 mW. In the literature, there exist many cantilever configurations. Beeby et al [13] designed and implemented a device with discrete magnets, coils and other components. In their system, the copper wires were thin such as 12  $\mu\text{m}$  in diameter. The volume was only 150  $\text{mm}^3$  and the harvester generated 46  $\mu\text{W}$  and 0.428 V at its resonance frequency.  $f = 52$  Hz. For the same configuration, Torah et al [14] obtained 58  $\mu\text{W}$  from the same excitation level by using larger magnets. In a different design, Buren and Troster [15] worked with a tubular translator with the cylindrical magnets and spacers. The device was operated with a vertical move by inducing voltages on the coils. The parallel springs produced vertical vibrations. The total volume of the device was 30.4  $\text{cm}^3$  and produced the averaged power of 35  $\mu\text{W}$ , when it was located on a moving knee. In another study, Yuen et al [16] has measured the power 120  $\mu\text{W}$  at 70.5 Hz. The proof mass moved inside a distance of 250  $\mu\text{m}$ . In the work of Hadas and his co-workers [17], they improved a wireless aircraft –monitoring system. Their device generated 3.5 mW at 34.5 Hz within the volume of 45  $\text{cm}^3$ . Their device was the largest one and used for different applications. In one of our most recent study [18], we have designed a new linear harvester with four small magnets and a movable core-coil system at the middle of them [18]. The moving body has been attached to the springs from two ends. In the experiments, the output peak voltage 0.75 V and the maximal peak power 14 mW have been achieved. That gives a power density of 0.3684  $\text{mW}/\text{cm}^3$ . The efficiency of this new design has reached to 36%.

In the present paper, a new EM linear harvester has been designed and the theoretical and experimental analyses have been performed. Section 2 gives the analytical analysis of the designed device. The next section gives the EM design and magnetostatic solutions of the proposed harvester. The experimental procedure is given in Section 4. The main findings, results and discussion are given in Section 5. Finally, the paper ends with a conclusion part to emphasize the vital results.

## 2. ANALYTICAL WORK

The proposed EM harvester is presented in Fig. 1. Both the EM and mechanical units are easy to construct. The device operates under a vertical mechanical excitation. All mechanical damping arises from the friction due to the movement inside the magnets.

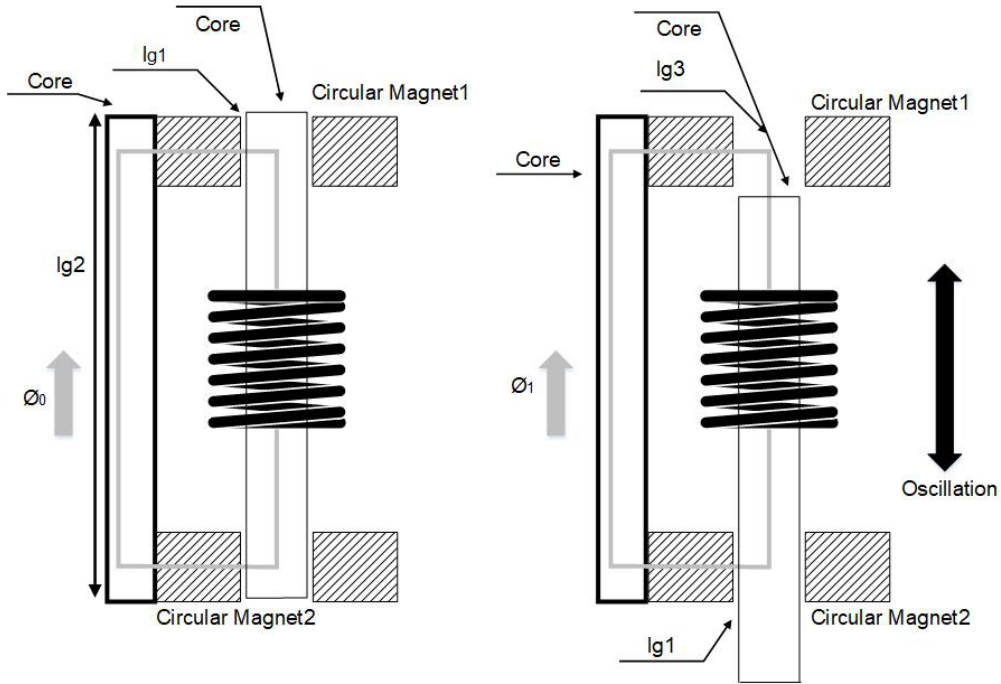


Figure 1. The sketch of the proposed EM harvester.

One spring wrapped the lower part of the core drives back and forth movement. The core is made of a steel nail. If the nail tip at the middle of the circular magnets moves upper part inside the upper circular magnet the air gap is minimized and caused a certain increase in flux through the flux path. That flux deviation would yield to a certain *EMF* at the terminals of the coil indicated as black at the middle of the nail.

The natural frequency of the system depends on total movable mass (i.e. the nail) without the coil and the spring coefficient. Since the mass of the coil is excluded in that system, that is innovative on that manner since the proof mass is small due to that reason. The stable coil also helps to get the voltage out of the terminals in a stable manner.

The theoretical approach starts with the equations of motion by following the sketches in Fig. 1. Then, the EM equations should be solved analytically. The harvester core carries the magnetic flux from one end of the core to the other end to complete the full path over the magnets. According to geometry, there also exists another core which is located outside the magnets indicated at the left hand-side of Fig. 1. Then the equations of motion are written as,

$$v = \frac{dz}{dt} \quad (1)$$

$$(m) \frac{dv}{dt} + \gamma v + \omega_0 z = A \cos(\Omega t) \quad (2)$$

for velocity and force variations depending on time. In the above expression,  $z$ ,  $v$ ,  $m$ ,  $\gamma$ ,  $\omega_0$  and  $\Omega$  denote displacement of the middle of core from the equilibrium point, velocity of the core, mass of the core, parasitic damping parameter, natural frequency and the excitation frequency, respectively.

In the EM process, the flux along a closed path should be determined for two cases in order to explain the magnetic circuit. Case I: The core is at the middle of the magnet pairs. Case II: It is out of the upper magnet. The reluctances over the flux path is defined as:

$$R_{tot}^{(1)} = R_{air}^{(1)} + R_{core}^{(1)} = \frac{2l_{g1}}{\mu_0 A} + \frac{2l_{g2}}{\mu_0 \mu_r A} \quad (3)$$

Here we neglect the length of radius of magnets since the magnets are too small compared to  $l_{g2}$ . The total reluctances are calculated over the paths of air media and the cores. The parameters  $l$  and  $A$  denote the length and cross sections of the materials in Fig. 1.  $A$  is defined by the area which is perpendicular to the flux direction inside the core.  $\mu_0$  and  $\mu_r$  show the magnetic permeability of air and the relative permeability of the cores, respectively. The upper index such as 1 denotes the Case 1, while 2 gives the Case 2. The flux expression is obtained of the calculation of the reluctance as follows [18]:

$$\Phi = \frac{F}{R_{tot}} \quad (4)$$

The expression above states that the magnetic flux  $\Phi$  can be obtained by dividing the magneto motive force  $F$  by the reluctance  $R_{tot}$ . The harvester has two magnets in 2 sides, therefore one can write,

$$\Phi^{(1)} = \frac{2F}{R_{net}^{(1)}} = \frac{\mu_0 \mu_r A F}{\mu_r l_{g1} + l_{g2}} \quad (5)$$

This formula defines the maximal flux along the flux path. For the Case 2, the reluctance changes due to  $l_{g3}$  as follows:

$$R_{tot}^{(2)} = R_{air}^{(2)} + R_{core}^{(2)} = \frac{l_{g1} + l_{g3}}{\mu_0 A} + \frac{2l_{g2} - l_{g3}}{\mu_0 \mu_r A} \quad (6)$$

For Case 2, one reads as,

$$\Phi^{(2)} = \frac{2F}{R_{tot}^{(2)}} = \frac{2F \mu_0 \mu_r A}{(\mu_r - 1) l_{g3} + 2l_{g2} + \mu_r l_{g1}} \quad (7)$$

by considering two magnets. For the determination of the flux difference between two cases, a subtraction between the cases are defined as,

$$\Delta \Phi = \Phi^{(1)} - \Phi^{(2)} = \frac{\mu_0 \mu_r A F}{\mu_r l_{g1} + l_{g2}} - \frac{2F \mu_0 \mu_r A}{(\mu_r - 1) l_{g3} + 2l_{g2} + \mu_r l_{g1}} \quad (8)$$

The simplification of the expression can be done as follows:

$$\Delta \Phi = \frac{l_{g3}(\mu_r - 1)F A \mu_0 \mu_r - l_{g1}F A \mu_0 \mu_r^2}{l_{g1}l_{g3}\mu_r (\mu_r - 1) + 3l_{g1}l_{g2}\mu_r + l_{g2}l_{g3}\mu_r + l_{g1}^2 \mu_r^2 - l_{g2}l_{g3} + 2l_{g2}^2} \quad (9)$$

Here, the formula between the flux linkage and electromotive force (*EMF*) is described by,

$$\varepsilon = -\frac{d\lambda}{dt} \quad (10)$$

Note that the flux linkage is as follows:

$$\lambda = N\Phi \quad (11)$$

The *EMF* is defined by,

$$\varepsilon = -N \frac{d\Phi}{dz} \frac{dz}{dt} \quad (12)$$

The formula above gives an opportunity to determine the position - dependent variation in *EMF*. Thereby, it is simplified by using velocity  $v$  as follows [18]:

$$\varepsilon = -Nv \frac{d\Phi}{dz} \quad (13)$$

Since the displacement in  $z$  is defined by  $l_{g3}$  in Eq. 11, one can transform the equation above into position - related form as  $l_{g3} = z$  for the analytical expression. Then Eq. 11 is transformed into,

$$\Delta\Phi = \frac{x(\mu_r - 1)FA\mu_0\mu_r - l_{g1}FA\mu_0\mu_r^2}{x l_{g1}\mu_r(\mu_r - 1) + 3l_{g1}l_{g2}\mu_r + x l_{g2}\mu_r + l_{g1}^2\mu_r^2 - x l_{g2} + 2l_{g2}^2} \quad (14)$$

After the derivation of the flux variation by displacement, one arrives at,

$$\frac{d\Phi}{dz} = \frac{((\mu_r - 1)FA\mu_0\mu_r)3l_{g1}l_{g2}\mu_r + l_{g1}^2\mu_r^2(\mu_r - 1)FA\mu_0\mu_r + (\mu_r - 1)FA\mu_0\mu_r 2l_{g2}^2 + l_{g1}FA\mu_0\mu_r^2 l_{g1}\mu_r(\mu_r - 1)}{[z(l_{g1}\mu_r(\mu_r - 1) + l_{g2}\mu_r - l_{g2}) + 3l_{g1}l_{g2}\mu_r + l_{g1}^2\mu_r^2 + 2l_{g2}^2]^2} + \frac{l_{g1}FA\mu_0\mu_r^2 l_{g2}\mu_r - l_{g1}FA\mu_0\mu_r^2 l_{g2}}{[z(l_{g1}\mu_r(\mu_r - 1) + l_{g2}\mu_r - l_{g2}) + 3l_{g1}l_{g2}\mu_r + l_{g1}^2\mu_r^2 + 2l_{g2}^2]^2} \quad (15)$$

For the total system equations,

$$\frac{dz}{dt} = v \quad (16)$$

$$\frac{dv}{dt} = -\frac{\gamma v}{(M + m)} - \frac{\omega_0^2 z}{(M + m)} + \frac{A}{(M + m)} \cos(\Omega t) \quad (17)$$

$$\frac{d\Phi}{dz} = \frac{((\mu_r - 1)FA\mu_0\mu_r)3l_{g1}l_{g2}\mu_r + l_{g1}^2\mu_r^2(\mu_r - 1)FA\mu_0\mu_r + (\mu_r - 1)FA\mu_0\mu_r 2l_{g2}^2 + l_{g1}FA\mu_0\mu_r^2 l_{g1}\mu_r (\mu_r - 1)}{[x(l_{g1}\mu_r(\mu_r - 1) + l_{g2}\mu_r - l_{g2}) + 3l_{g1}l_{g2}\mu_r + l_{g1}^2\mu_r^2 + 2l_{g2}^2]^2} + \frac{l_{g1}FA\mu_0\mu_r^2 l_{g2}\mu_r - l_{g1}FA\mu_0\mu_r^2 l_{g2}}{[x(l_{g1}\mu_r(\mu_r - 1) + l_{g2}\mu_r - l_{g2}) + 3l_{g1}l_{g2}\mu_r + l_{g1}^2\mu_r^2 + 2l_{g2}^2]^2} \quad (18)$$

$$\varepsilon = -Nv \frac{d\Phi}{dz} \quad (19)$$

are obtained. In these final equations,  $\phi$ ,  $F$ ,  $A$ ,  $l_g$ ,  $\mu$ ,  $N$ ,  $v$ , and  $z$  denotes flux, *mmf*, section of core, air gap, permeability, winding number, velocity and moving direction, respectively.

### 3. EM ANALYSIS

Fig. 2 shows the EM design of the proposed linear harvester. Here the magnets and the cores are represented by green and blue, respectively. The winding is shown by the yellow coil and attached on the core. The moving axis is in  $z$ -direction and the system is stable in  $x$  and  $y$  direction.

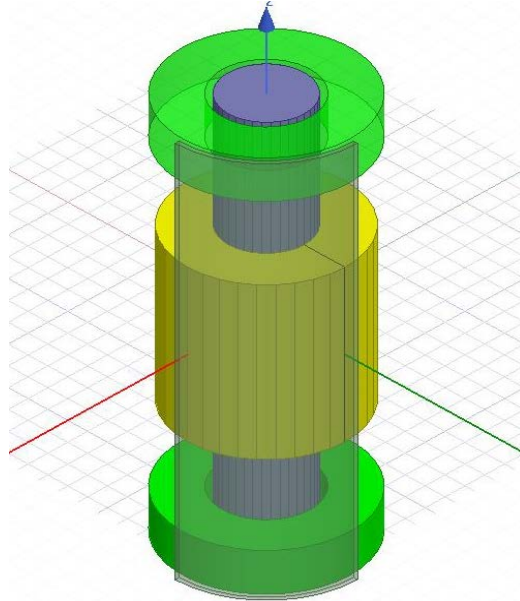


Figure 2. The EM design of the proposed harvester

The core moves up and down with the winding together and the difference on the magnetic flux creates an electromotive force between the terminals of the coil. Fig. 3 shows the magnetic field strength ( $H$ ) of the harvester in its equilibrium point. Note that the magnetic field strength maximizes inside the magnets at the upper and lower part of the device, and it gives moderate values inside the core and minimizes far away the magnets. The airgap between the inner part of the magnet and the core should be minimized for high magnetic flux density. Therefore, the core should be located very close to the inner part of the magnets.

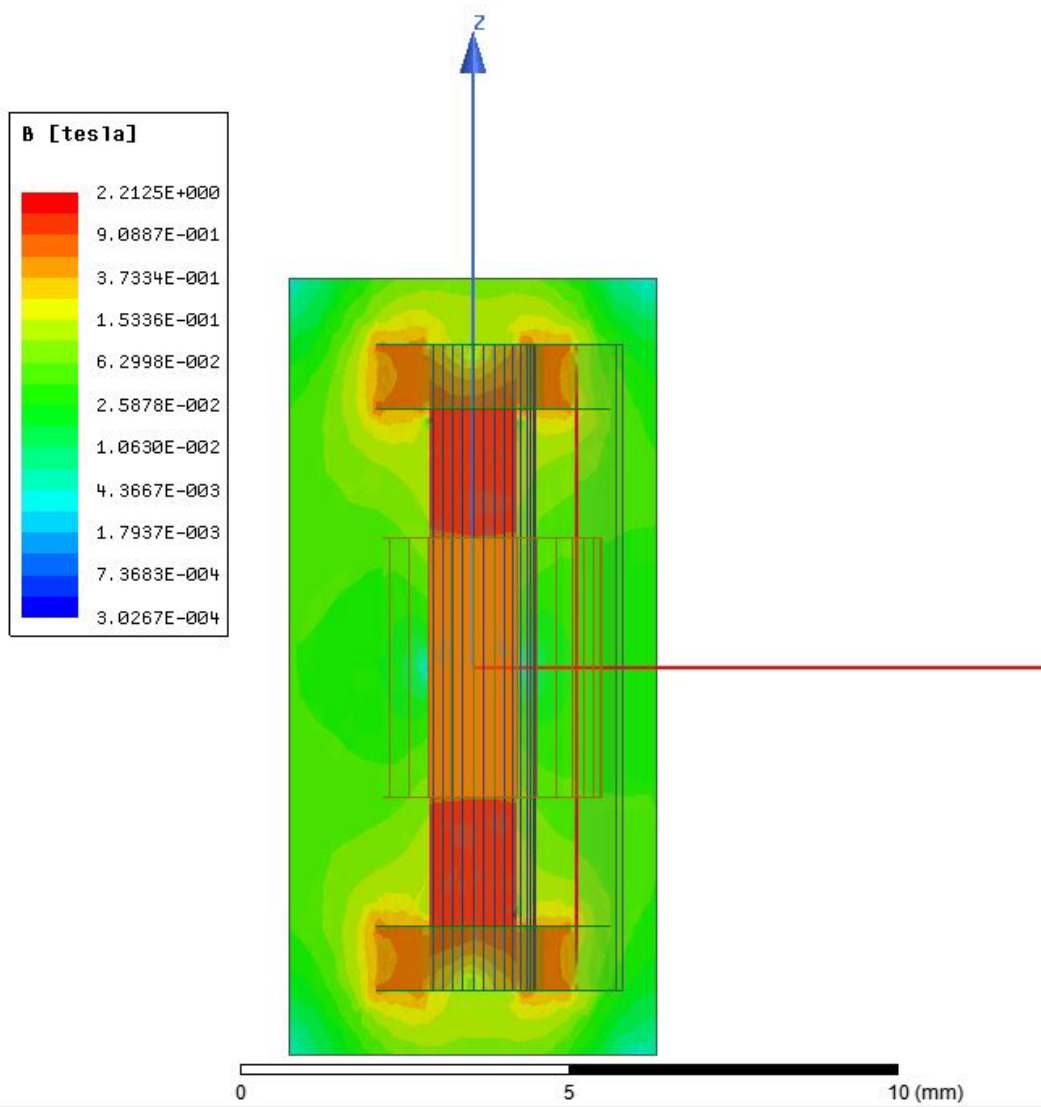


Figure 3. The magnetic field strength (i.e.  $H$ ).

The winding length should be optimized via the largest equilibrium location from the moving tip. Since the movement will be back and forth in  $z$ -direction, the coil length should be restricted, however the volume of the coil also determines the current flowing through the cross section of the coil, thereby it affects the electromotive force generated from the system.

In Fig. 4, the magnetic flux density (i.e.  $B$ ) is shown. It is obvious that the flux from down to up circulates inside the core by giving a high value around 0.8 T. This value can also be increased by adjusting the smaller airgaps between the inner side of the magnets and the core, whereas, 1 mm airgap is sufficient for the present application.

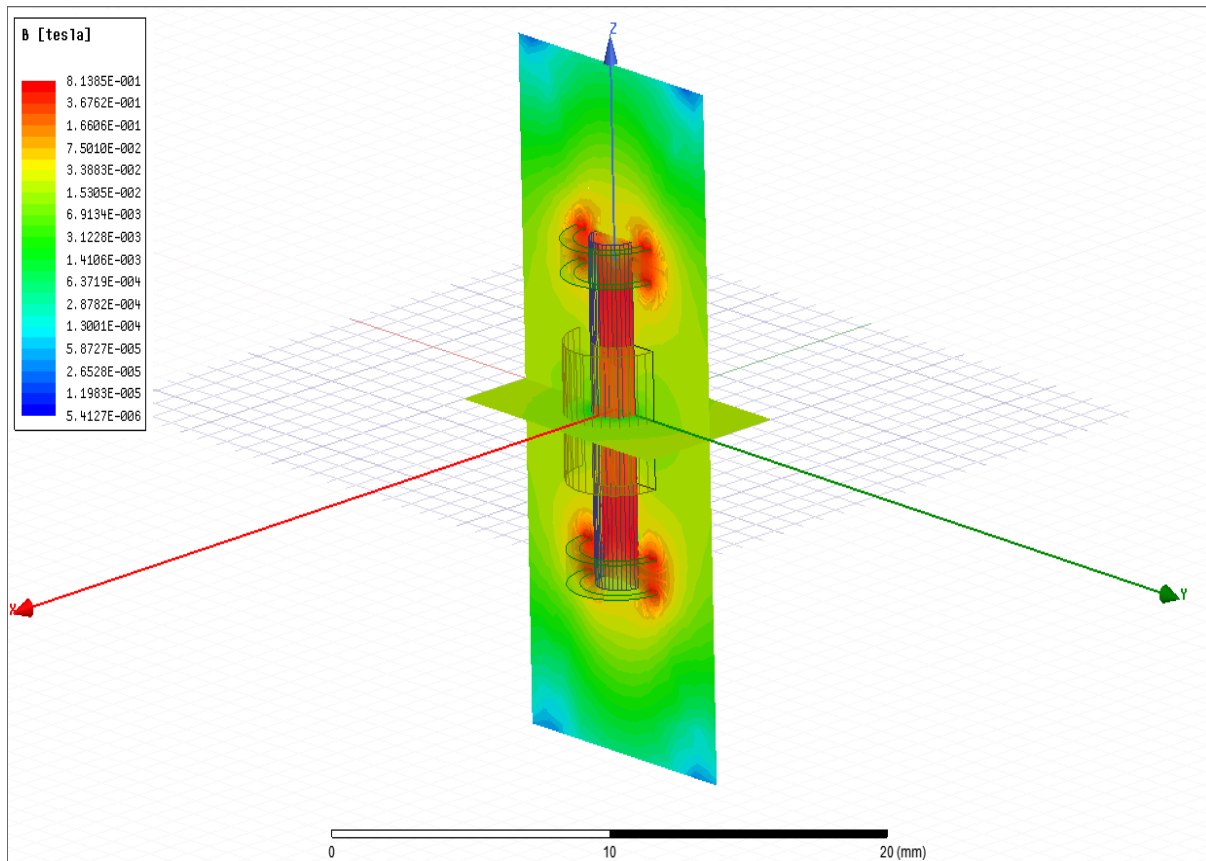
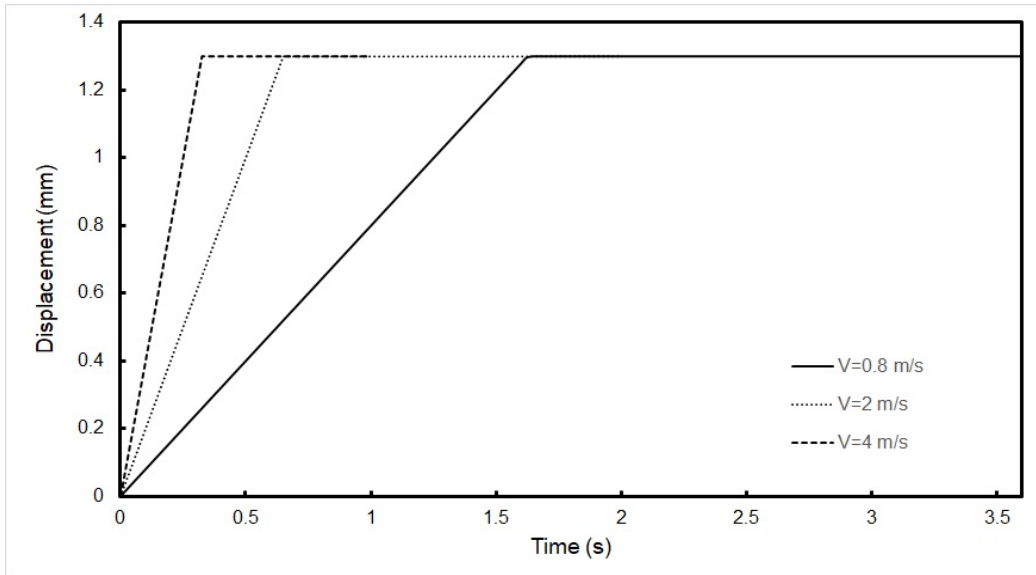


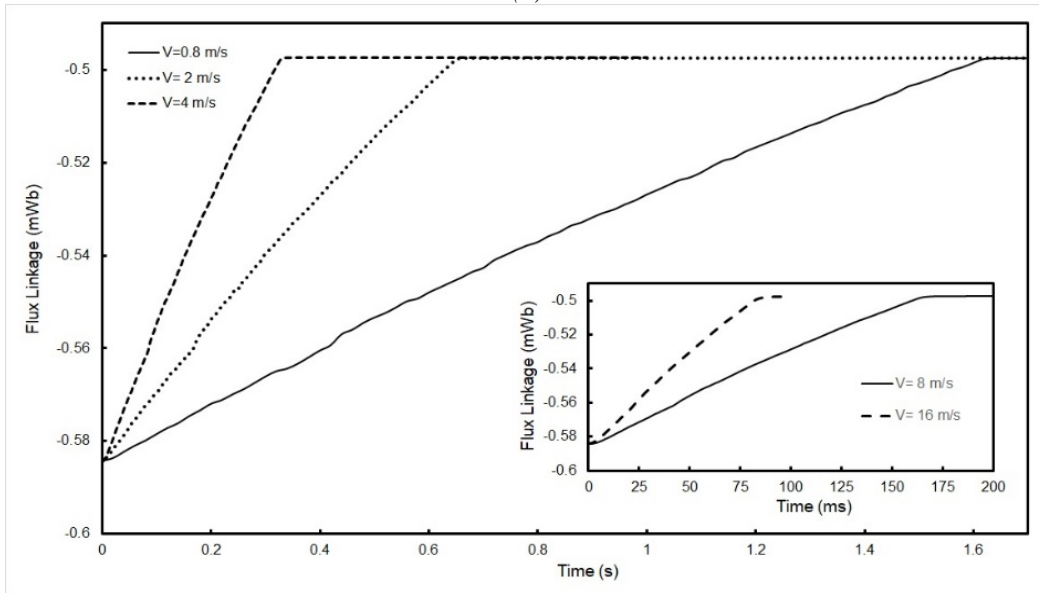
Figure 4. The magnetic flux density (i.e.  $B$ )

Note that the flux of the cylindrical magnets is also completed onward from its inner to outer sides as seen in the tip of the core. It proves that if the core is taken away with a 1-3 cm, the flux flowing inside the core will be decreased or stopped. That reality drives that harvester to generate the electricity.

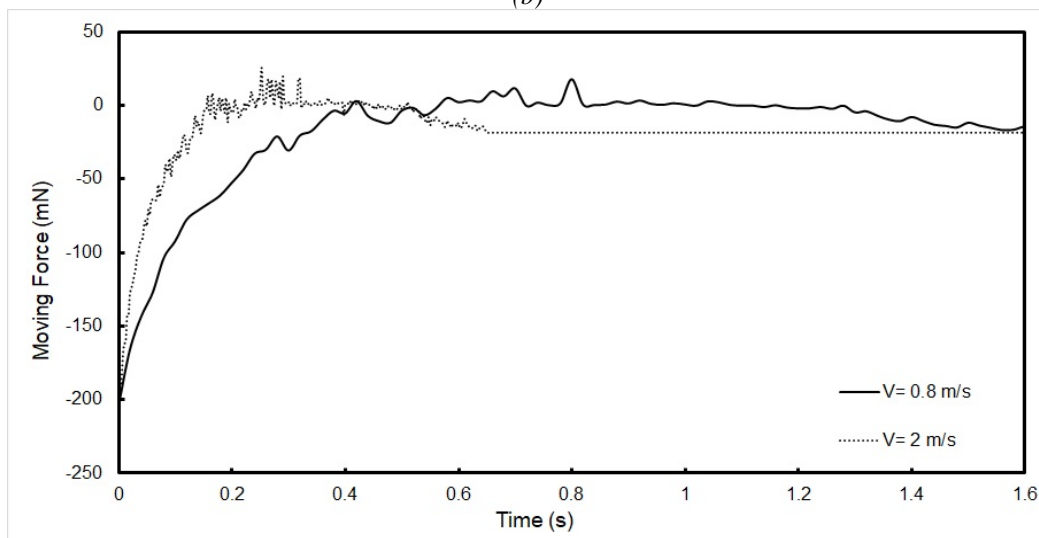
The results of magneto dynamic analyses are shown in Fig 5(a-e). For the time-dependent solutions, the geometry shown in Fig. 2 has been used in a certain moving body volume. For the moving part, the combination of core and coil is used. The maximal displacement in Fig. 5(a) has been adjusted as 1.3 mm for 0.8 m/s, 2 m/s and 4 m/s speed values. When the speed increases, the equilibrium position comes back earlier with the value 0.3 s. The change in flux linkage is given in Fig. 5(b). With a constant speed, the change in the fluxes are linear. It changes from 0.495 mWb to 0.585 mWb. For high speeds, the increase becomes suddenly as in the inset of Fig. 5(b). When the core moves inside the domain, a certain change in magnetic force occurs as in Fig. 5(c). When the core tip and magnet are closed to each other, 200 mN magnetic force is sufficient to make an oscillation back and forth. The increase in speed yields to zero force case earlier reasonably. The induced voltages are calculated according to the Faraday's law (Fig. 5(d)). For that the winding volume, wire diameter, conductance of the wire and the change in flux linkage play important role. For instance, 60  $\mu\text{V}$ , 150  $\mu\text{V}$  and 300  $\mu\text{V}$  voltages can be obtained for 0.8 m/s, 2 m/s and 4 m/s speeds, respectively. These voltages are determined via an external circuit and the code calculate the voltage over the windings and gives that voltage to the equivalent resistor loaded circuit, where the winding terminals are directly connected. Note that the current values can also be measured internally when the resistive load is connected to the winding terminals. According to Fig. 5(e), 110  $\mu\text{A}$  and 300  $\mu\text{A}$  are available for 0.8 m/s and 2 m/s speeds.



(a)



(b)



(c)

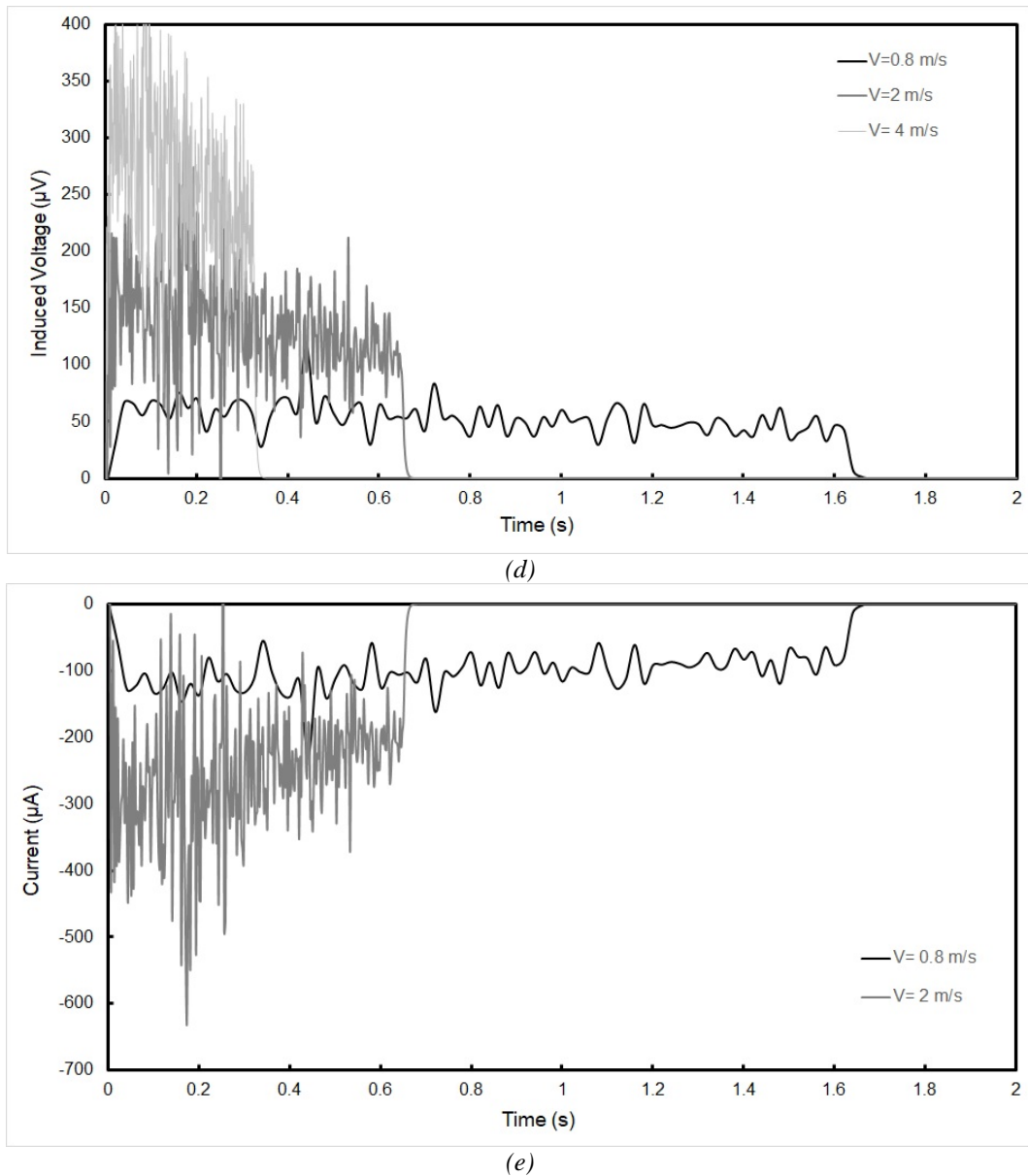


Figure 5. The time-dependent EM simulation of the harvester depicted in Fig. 2: (a) Displacement from the equilibrium position for three different speeds, (b) flux linkages for various speeds, (c) The magnetic force between the core and magnet, (d) induced voltage over the coil, (e) current flowing through a single core wire when  $R_L = 0.2 \Omega$  is used.

These voltage and current values are in good agreement with the experiments and if the air gaps are optimized according to the experiments, the values are expected to be same with the experimental values for all speeds.

### 3. EXPERIMENTAL

Fig. 6 shows the experimental setup including the harvester located on the top of the shaker and the measurement tools. In detail, the setup includes a signal generator for the external excitation of the shaker with a certain frequency and amplitude for frequency responses. An amplifier is required in order to enhance the excitation magnitude for the shaker. In addition, a variable electrical load table is used

for the detection of optimized power generation depending on the frequencies. A Data Acquisition (DAQ) card is also used in order to export the results of data to a laptop.

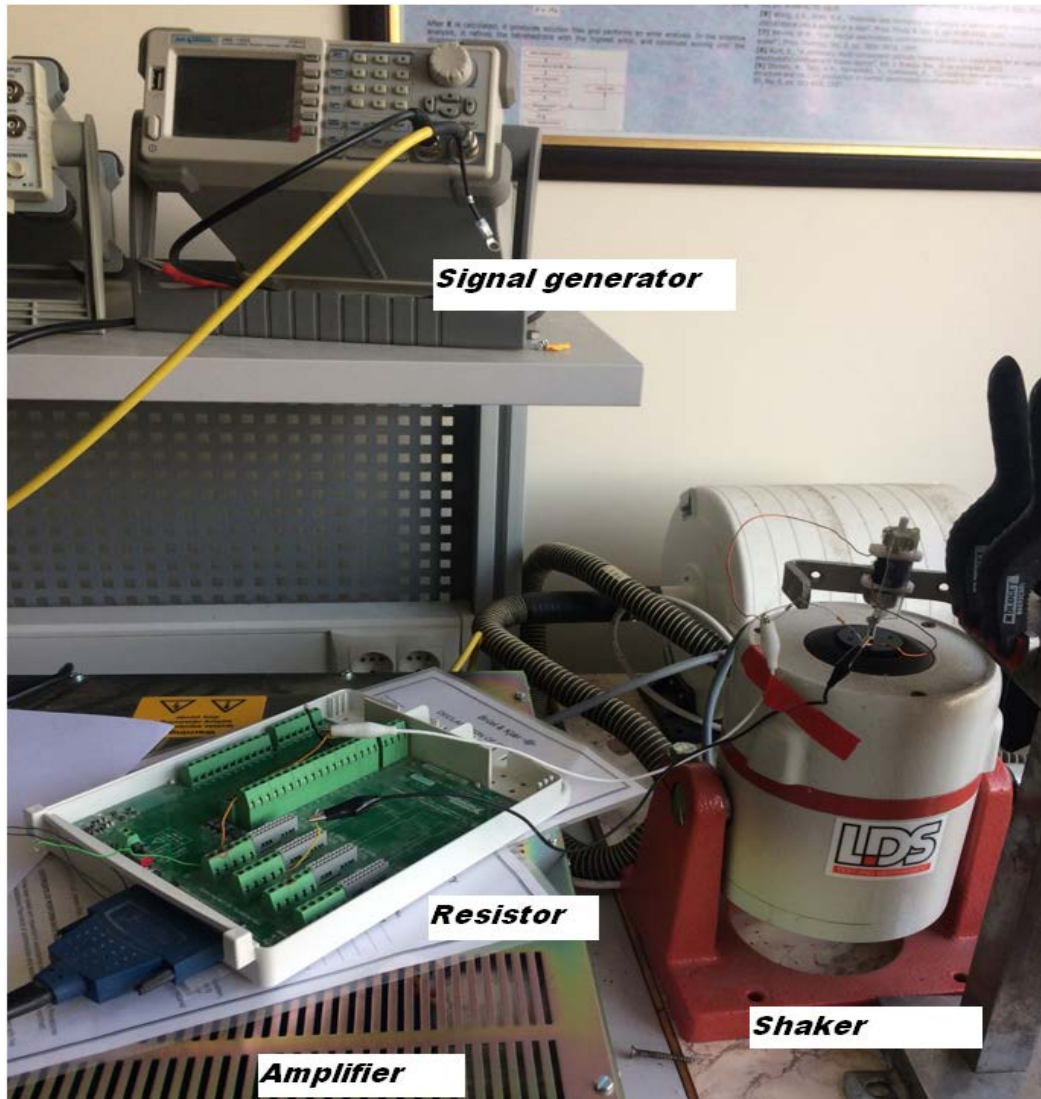


Figure 6. The vibration test setup for the proposed EM harvester.

The DAQ card used in the experimental studies is NI USB-6250 type. It has 16 analog inputs, that is already sufficient for such a study. The card achieves to make multiple recordings of the data such as the displacement of the core end and generated voltages. The data is collected via a LabVIEW package during the tests. A sensor head can measure the oscillations with a sampling rate of  $t = 1$  ms. For the shaker unit, a signal generator AWG-1020 type and an amplifier/ shaker combination LDS V406 are used. This shaker system can produce vibrations from 1 Hz to 1kHz in desired amplitudes. Note that the shaker is only used for the frequency responses of the new device. Therefore, an efficiency study is not reasonable for such a testing study. However, one can make an estimation by considering the mechanical power as input power and its conversion to the electrical power as output power. For instance, Hendijanizadeh et al [19] has proved that such an efficiency for any linear EM harvester cannot even reach to 50% because of the low conversion ratio of the mechanical power. This conversion ratio can be increased further in the rotating systems rather than the linear structures. According to literature [1,10,12,19], it is clear that the efficiency values of many harvesters are stated around 20%, for instance, in one of our recent designs, the efficiency 36% has been achieved [18]. Besides, many harvesters can have low efficiencies such as 20% and there also exists special designed devices such as ASP 400 and Micro-mega with the efficiencies 40% and 30%, respectively in the literature.

4. EXPERIMENTAL RESULTS AND DISCUSSION

The designed and implemented EM harvester is shown in Fig. 7(a). The device has two circular high flux density rare-earth magnets (i.e. Nd<sub>2</sub>Fe<sub>14</sub>B) with 18 mm diameter and 10 mm thickness mounted from one side of the harvester. The characteristic *B-H* curve of the steel nail is shown in Fig. 7(b), where the knee flux density is about 1.5 T. A coil is wound the core. The terminals can transmit the electricity out of the harvester without any physical difficulty since the displacement does not exceed 5 mm at its maximum displacement. The dimensions of the harvesters are 2.4 x 2.4 x 6 cm<sup>3</sup>.

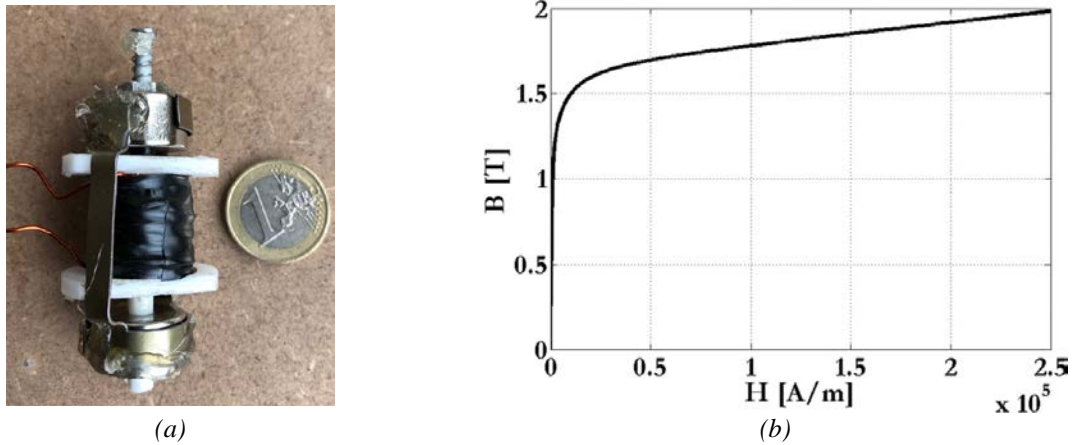
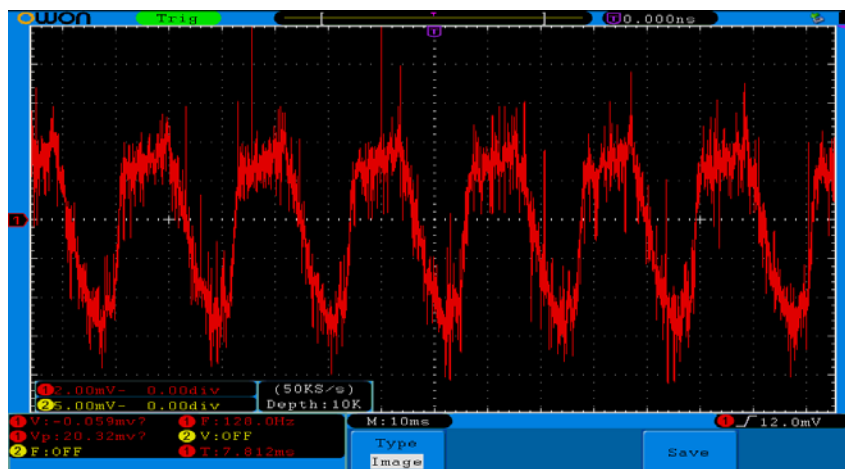
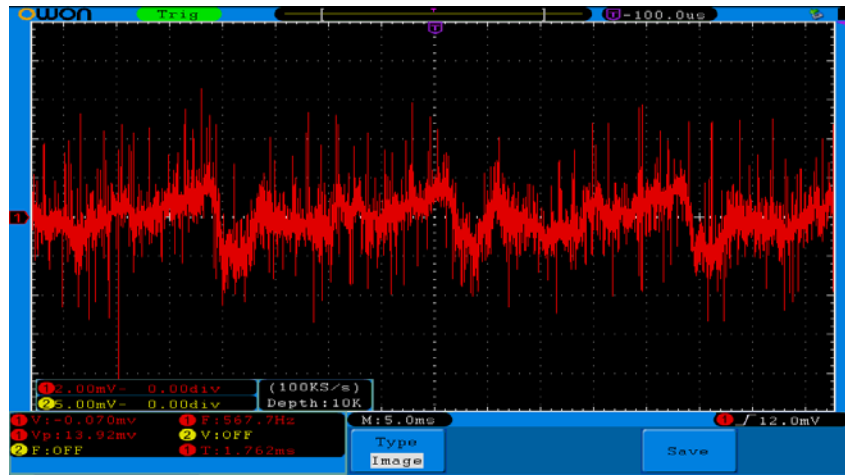


Figure 7. (a) The proposed EM harvester attached to test setup. (b) The characteristic *B-H* curve of the core nail.

When the oscillation occurs experimentally, the spring enforces the nail back and forth inside the magnets depending on the external frequency. The maximal amplitude is obtained for the natural frequency of the system according to the literature. Fig. 8(a-b) shows the sample voltage waveforms from the shaker tests. For the clarity, we put only the results of an electrical load of 0.1 Ohms. The waveform dramatically changes with the test frequency. Although the displacement of shaker occurs in an ideal sinusoidal form, the output waveforms have high harmonic distortion as we have encountered in many harvester systems [4]. The peak voltages have been measured as 20 mV as in Fig. 8(a) and 13 mV as in Fig. 8(b).



(a)



(b)

Figure 8. Output waveforms from the terminals of harvester: (a) without load and  $f=58$  Hz, (b) with  $R_L=0.1 \Omega$  and  $f=55$  Hz.

In Fig. 9, the power plots are represented for various excitation frequencies. The power scale is around  $25 \mu\text{W}$  and changes by frequency. The maximal power has been obtained for 44 Hz, when the electrical load is adjusted as 0.2 Ohm. However, the system generates  $25 \mu\text{W}$  around 14 Hz for 0.1 Ohm. There is also a wide power generation band between 25 Hz and 40 Hz with the averaged value of  $10 \mu\text{W}$ . After the airgap optimization of the harvester, that power amount should certainly be increased upto several hundred Watts. In order to give a comprehensive idea among the other designed and produced harvesters, Fig. 10 has been plotted. Note that the features of all black points can be obtained from Ref. [9]. Whereas the blue and red colored ones indicate the resonant frequency and scaling length values of present designed device and one of our recent designed one [18]. The electromechanical harvester systems always give a theoretical value between two lines as indicated in Fig. 10.

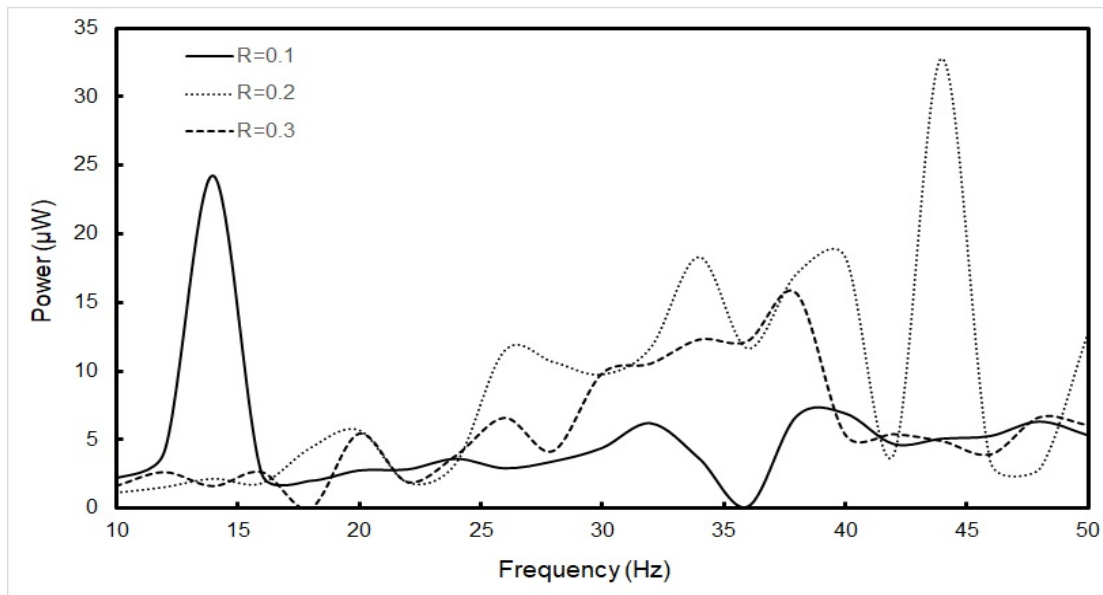


Figure 9. Maximal power plots versus excitation frequency for various electrical loads.

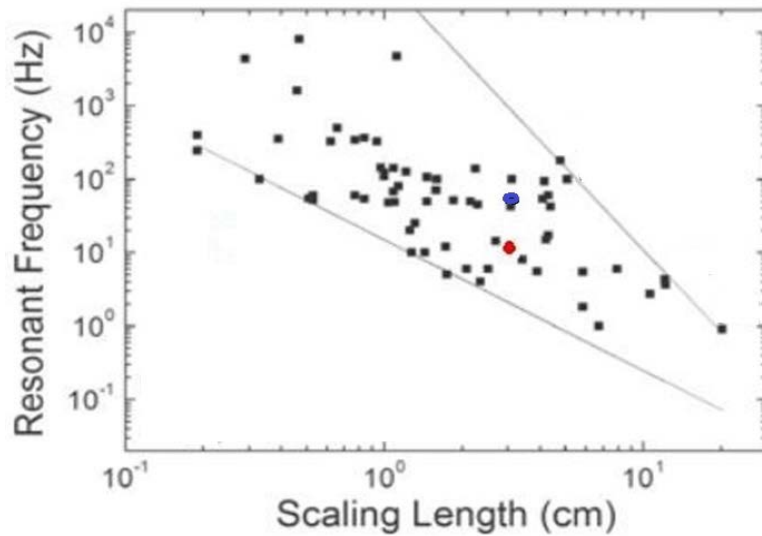


Figure 10. The characteristic resonant frequencies of the harvester's world-wide. The present device and the recent one of Kurt et al [18] are shown via blue and red points, respectively. The information on other devices can be obtained from Ref. [9].

The resonant frequency cannot be lower or higher from a certain value for a special scaling length. Here, the scaling length is nothing else than the measure of the device dimension. The increase in the dimension can yield to lower frequencies. The present design is at the middle region of the diagram in that respect.

## 5. CONCLUSIONS

The designed EM harvester is a micro-scaled power generating device and useful for medium volume required applications. The analytical expressions have proven that a certain electromotive force is available due to the variation in  $z$  direction of the core. An electromotive force can be obtained via the displacement of the core tip inside the cylindrical magnets inside the moving volume. The EM analyses with magneto static and magneto dynamic scales have shown that the new designed device has a 0.8 T flux density inside the core. When this flux density changes by time, certain voltage over the coil occurs in that geometry in microvolt scale. When a resistive load is attached to the terminal of the device, certain current value in  $\mu\text{A}$  scale flows over the load. According to the experimental tests, this compact harvester generates  $P = 20 \mu\text{W}$  maximal power under 44 Hz within the amplitude of 5 mm. The optimal power has been measured for 0.2 Ohm, experimentally. For the future study, the power scale will be increased by using better core structures and air gap optimization, however such systems have energy scales with the coil volume. That reality enforces us to design the harvester according to its usage aim and environment.

## REFERENCES

- [1] Beeby, S. P., O'Donnell, T. Electromagnetic Energy Harvesting, In *Energy Harvesting Technologies* (Editors: S. Priya, D.J. Inman), Springer, USA, 129 (2009).
- [2] Uzun, Y., Kurt, E., Kurt, H.H., Explorations of displacement and velocity nonlinearities and their effects to power of a magnetically-excited piezoelectric pendulum, *Sensors and Actuators A: Physical*, 224, 119 (2015).

- [3] Uzun, Y., Kurt, E., The effect of periodic magnetic force on a piezoelectric energy harvester, *Sensors and Actuators A: Physical*, 192, 58 (2013).
- [4] Bizon, N., Tabatabaei, N.M., Blaabjerg, F., Kurt, E., *Energy Harvesting and Energy Efficiency: Technology, Methods, and Applications*, Springer, Switzerland, 107 (2017).
- [5] Kurt, E., Gor, H., Doner, U., Electromagnetic design of a new axial and radial flux generator with the rotor back-irons, *International Journal of Hydrogen Energy*, 41(17), 7019 (2016).
- [6] Arslan, S., Kurt, E., Akizu, O., Lopez-Guede, J.M., Design optimization study of a torus type axial flux machine. *Journal of Energy Systems*, 2(2): 43-56, (2018), DOI: 10.30521/jes. 408179
- [7] Celik, K., Kurt, E., Uzun, Y., Experimental and theoretical explorations on the buckling piezoelectric layer under magnetic excitation, *Journal of Electronic Materials*, 46(7), 4003 (2017).
- [8] Kurt, E., Cottone, F., Uzun, Y., Orfei, F., Mattarelli, F., Özhan, D., Design and implementation of a new contactless triple piezoelectrics wind energy harvester, *Int. J. Hydrogen Energy*, 42(28), 17813 (2017).
- [9] Spremann, D., Manoli, Y., *Electromagnetic vibration energy harvesting devices: Architectures, design, modeling and optimization* (Vol. 35). Springer Science & Business Media (2012).
- [10] Amirtharajah, R., Chandrakasan, A.P., Self-powered signal processing using vibration-based power generation, *IEEE Journal of Solid-State Circuits*, 33(5), 687 (1998).
- [11] El-Hami, M., Glynne-Jones, P., White, N.M., Hill, M., Beeby, S., James, E., Brown, A.D., Ross, J.N., Design and fabrication of a new vibration-based electromechanical power generator”, *Sensors and Actuators A: Physical*, 92(1), 335 (2001).
- [12] Glynne-Jones, P., Tudor, M.J., Beeby, S.P., White, N.M., An electromagnetic, vibration-powered generator for intelligent sensor systems, *Sensors and Actuators A: Physical*, 110(1), 344 (2004).
- [13] Beeby, S.P., Tudor, M.J., White, N.M. Energy harvesting vibration sources for microsystems applications, *Measurement Science and Technology*, 17, R175 (2006).
- [14] Torah, R.N., Glynne-Jones, P., Tudor, M.J., Beeby, S.P. Energy aware wireless microsystem powered by vibration energy system, *Pro. 7<sup>th</sup> Int. Workshop on Micro and Nanotechnology for Power Generation and Energy Conversion Applications (PowerMEMS 2007)*, Freiburg, Germany, 323, 28-29 Nov. (2007).
- [15] Von Büren, T., Tröster, G., Design and optimization of a linear vibration-driven electromagnetic micro-power generator, *Sensors and Actuators A: Physical*, 135(2), 765 (2007).
- [16] Yuen, S.C., Lee, J.M., Li, W.J., Leong, P.H. An AA-Sized Vibration-Based Microgenerator for Wireless Sensors, *IEEE Pervasive Computing*, 6(1), 64 (2007).
- [17] Hadas, Z., Kurfurst, J., Ondrusek, C., Singule, V., Artificial intelligence based optimisation for vibration energy harvesting applications, *Microsystem Technologies*, 1–12, (2012), DOI: 10.1007/s00542-012-1432-1
- [18] Kurt, E., Kale, M.M., Akbaba, S., Bizon, N., Analytical and experimental studies on a new linear energy harvester, *Canadian J. Physics*, 2018, <https://doi.org/10.1139/cjp-2017-0708>.
- [19] Hendijanizadeh, M., Sharkh, S.M., Elliott, S.J., Moshrefi-Torbati, M. Output power and efficiency of electromagnetic energy harvesting systems with constrained range of motion, *Smart Materials and Structures*, 22:125009 (2013).